Interpenetrated Magnesium–Tricalcium Phosphate Composite: Manufacture, Characterization and In Vitro Degradation Test

Mariano Casas-Luna, Serhii Tkachenko, Miroslava Horynová, Lenka Klakurková, Pavel Gejdos, Sebastian Diaz-de-la-Torre, Ladislav Celko, Jozef Kaiser, Edgar B. Montufar

Acta Metallurgica Sinica (English Letters)
Volume 30, issue 4, pp. 319-325

Print ISSN: 1006-7191
Online ISSN: 2194-1289

DOI: http://dx.doi.org/10.1007/s40195-017-0560-0

Version: accepted manuscript

Interpenetrated Magnesium–Tricalcium Phosphate Composite: Manufacture, Characterization and In Vitro Degradation Test

Mariano Casas-Luna[1] · Serhii Tkachenko[1] · Miroslava Horynová[1] · Lenka Klakurková[1] · Pavel Gejdos[1] · Sebastian Diaz-de-la-Torre[2] · Ladislav Celko[1] · Jozef Kaiser[1] · Edgar B. Montufar[1]

Received: 24 February 2017 / Revised: 28 February 2017 / Published online: 9 March 2017

Abstract Magnesium and calcium phosphates composites are promising biomaterials to create biodegradable load-bearing implants for bone regeneration. The present investigation is focused on the design of an interpenetrated magnesium–tricalcium phosphate (Mg–TCP) composite and its evaluation under immersion test. In the study, TCP porous preforms were fabricated by robocasting to have a prefect control of porosity and pore size and later infiltrated with pure commercial Mg through current-assisted metal infiltration (CAMI) technique. The microstructure, composition, distribution of phases and degradation of the composite under physiological simulated conditions were analysed by scanning electron microscopy, elemental chemical analysis and X-ray diffraction. The results revealed that robocast TCP preforms were full infiltrated by magnesium through CAMI, even small pores below 2 μm have been filled with Mg, giving to the composite a good interpenetration. The degradation rate of the Mg–TCP composite displays lower value compared to the one of pure Mg during the first 24 h of immersion test.

KEY WORDS: Calcium phosphate; Magnesium; Liquid metal infiltration; Spark plasma sintering; Corrosion

1 Introduction

Recently new types of metallic and calcium phosphate biodegradable composites are gaining attraction for the fabrication of osteosynthetic implants [1–3]. The driving force is to increase the mechanical strength of the calcium phosphate, without scarifying its degradability and osteoconductivity [4, 5]. Among the different biodegradable metals available, magnesium appears as the best alternative due to its good tolerance in human body, its osteogenic effect and mechanical properties similar to the human bone [6–8]. Nevertheless, the degradation rate of pure magnesium is faster than bone regenerative capacity and several works are focused to increase its corrosion resistance in biological environment [7, 9–12]. On the other hand, calcium phosphates, such as hydroxyapatite (HA) or tricalcium phosphate (TCP) have been widely investigated and used as bioactive materials [5, 13–15]. The bone regenerative capacity of calcium phosphates is considerably improved by the incorporation of macro-pores in their structure [16]. Because of this, several works have been devoted to fabricate macro-porous calcium phosphate materials [17–19]. Recently additive manufacturing methods have been also explored for such aim [20–22]. Among the different tested methods, the direct ink writing or robocasting is one of the most promising alternatives [20, 23]. In this process, an ink based on the powder of the material of interest is prepared by the incorporation of a binder material, mainly a polymer. Afterwards the ink is

Available online at http://link.springer.com/journal/40195

✉ Edgar B. Montufar
eb.montufar@ceitec.vutbr.cz

[1] CEITEC - Central European Institute of Technology, Brno University of Technology, Purkyňova 656/123, 612 00 Brno, Czech Republic

[2] CIITEC - Centro de Investigación e Innovación Tecnológica, Instituto Politécnico Nacional, Cerrada de CECATI, 02250 Mexico City, Mexico

placed into a syringe and loaded in the robocasting device which controls the displacement of the syringe to print a desired pattern previously designed in silico. HA and TCP structures with controlled porosity can be produce with robocasting [10, 24–26]. However, the main drawback of porous calcium phosphates is their low mechanical strength and toughness due to their ceramic nature. This impairs their application in treatment of bone defects under load-bearing conditions. Different methods have been developed to produce magnesium–calcium phosphate composite materials that overcome this problem. For example, common powder metallurgy routs are used to produce particle reinforced composites, with either magnesium or calcium phosphate matrix.

A high-performance type of composites are the interpenetrated composites. In those materials, both the matrix and the reinforcement form a continuous three-dimensional network in the material [27]. Most of the interpenetrated composites are fabricated by metal infiltration of the porous ceramic preforms [28, 29], having as a limitation the mechanical strength of the preform because nearly all of those techniques apply high pressure to ensure the infiltration of the metal in the porosity of the ceramic [29].

In the present work, a new pressure less infiltration method is explored. The process named current-assisted metal infiltration (CAMI) uses the principle of spark plasma sintering [30, 31] to melt magnesium under vacuum, and after melting liquid magnesium infiltrates the ceramic preform by gravity. The process has the advantage of the fast heating rate of the material due to pulsed electric current discharges, allowing infiltration in a few minutes. In addition to the introduction of this novel infiltration technique, this work presents the advantage of robocasting to produce TCP preforms with well-controlled, reproducible and well-defined architecture. The chemical and structural characterization of the interpenetrated composite is performed and its degradation rate under simulated physiological conditions is studied as an initial attempt to use such composite as a resorbable biomaterial.

2 Materials and Methods

2.1 Direct Ink Writing of Tricalcium Phosphate

Commercial TCP powder (VWR Chemicals, Belgium) and 30% w/w Pluronic F–127 (Sigma Aldrich, Germany) solution in distilled water were homogeneously mixed in a liquid to a powder ratio of 0.6 g of Pluronic solution per gram of TCP powder, in order to produce the ink for robocasting. The ink was loaded into a commercial syringe (Optimum® syringe barrels, Nordson EFD) and placed in the printing head of a direct ink writing system (Pastecaster, Spain). Immediately, cylindrical porous preforms with 7.5 mm in diameter and 15 mm in height were printed in the air at room temperature at a speed of 8 mm/min using tapering tips with an internal aperture of 250 μm. The final samples presented pores of 350 μm, formed by the distance between adjacent TCP filaments on the same plane (distance from filament surface to filament surface). Filaments were orthogonal between adjacent planes to form a parallel grid.

After manufacture, the preforms were dried at room temperature for 24 h and placed into a furnace (LH30/13, LAC, Czech Republic), to be sintered at 1100 °C during 5 h. While the chemical composition of the preforms was determined by X-ray diffraction (XRD; Rigaku SmartLab 3 kW) using Cu-radiation, the microstructure was observed by scanning electron microscopy (SEM; LYRA3 XMU, TESCAN) in samples previously coated with carbon to prevent electrical charging during observation.

2.2 Current-Assisted Magnesium Infiltration

Five grams of pure commercial magnesium powder (Riedel-de Haën S030195, Germany) were pre-compacted at 7 kN at room temperature to obtain a green disc of 20 mm in diameter. Afterwards, the magnesium discs were placed inside a graphite die designed for infiltration. Briefly, the die was 5 mm in external diameter and 5 mm of length. The top part of the die had an inner diameter of 20 mm, where the magnesium pre-compacted disc was placed, and the bottom part had an inner diameter of 10 mm, where the TCP preform was placed. The bottom aperture of the die was sealed with a graphite lid that worked as a bottom punch for conducting the electrical current. In the top part, the die was sealed with a 20-mm punch protruded from the die. The infiltration of magnesium was performed in a spark plasma sintering apparatus (SPS, Dr. Sinter 1050, Japan), using the CAMI variant of the technique. After placing the die set into the equipment, the electrical circuit was closed applying a constant mechanical load of 1 kN. Due to the design, the mechanical load was supported by the die instead than the TCP preform. Then, the melting of magnesium and the infiltration were performed by heating the die at a heating rate of 100 °C min^{-1} to 670 °C and 1 min of dwell time under vacuum. The heating was achieved by applying a direct electrical current discharge at on–off cycles of 12 and 2 ms, respectively. The final cylindrical samples had dimensions of 10 mm in diameter and a variable height of around 20 mm.

For the microstructure observation and phase composition characterization, samples were longitudinally cut and polished with SiC abrasive paper and diamond suspension till 1 μm finish. The microstructure was analysed by SEM and energy-dispersive X-ray spectroscopy to see the

elemental distribution of the phases and to determine any phase transformation or reactions between the ceramic and metallic phases. The crystalline phase composition of the composite was determined by XRD.

2.3 In Vitro Degradation Test

Infiltrated samples were cut into discs of 10 mm in diameter and 2 mm height to perform the in vitro degradation test. The discs were polished until 2400-grit SiC sand paper, cleaned with isopropanol, dried in air and immersed in saline solution (0.9 wt% NaCl in distilled water) at 37 °C. The volume of saline solution used for the test was fixed to maintain a sample surface-to-volume ratio of 9 mm^2 ml^{-1}. As reference material, magnesium discs were cut from a commercial pure magnesium bar (99.9%, 12.7 mm in diameter, MG007924, Goodfellow, UK). The degradation of the samples was monitored at 3, 6, 12, and 24 h. After each time, the formed corrosion products were removed by treating the corroded disc with chromic oxide and silver nitrate solution (ISO 8407:2009(E)). The weight change was registered. Then, the degradation rate (DR) was determined in mm $year^{-1}$ by the following equation:

$$DR = 8.76 \times 10^4 \frac{\Delta W}{S \cdot \tau \cdot \rho}. \quad (1)$$

where ΔW is the weight change in g after the immersion time; S stands for the surface area of the disc sample in cm^2; τ is the immersion time in saline solution, expressed in h; and ρ is the bulk density of the specimens in g cm^{-3} (average value of 1.76 ± 0.04 g cm^{-3} for the composite and 1.74 g cm^{-3} for pure magnesium).

3 Results and Discussion

Robocast TCP preforms with a parallel grid structure and macro-pores of 350 μm can be observed in Fig. 1a. The microstructure of the sintered filaments is presented in Fig. 1b. The filaments present the typical microstructure of sintered TCP ceramics with small micro-pores, with average size below 2 μm and homogenous distribution. XRD (Fig. 1c) confirms the purity of the preforms, presenting only the diffraction peaks for TCP phase.

After conventional sintering, the preforms were infiltrated with magnesium using the newly developed CAMI technique. After extraction from the die, the samples had the shape of a screw with a diameter in the thinner part of 1 and 2 cm of diameter in the head (Fig. 2a). The head consisted basically of excess of magnesium used for infiltration. In contrast, the thinner shaft of the sample contains the infiltrated preform in the tip and excess of magnesium

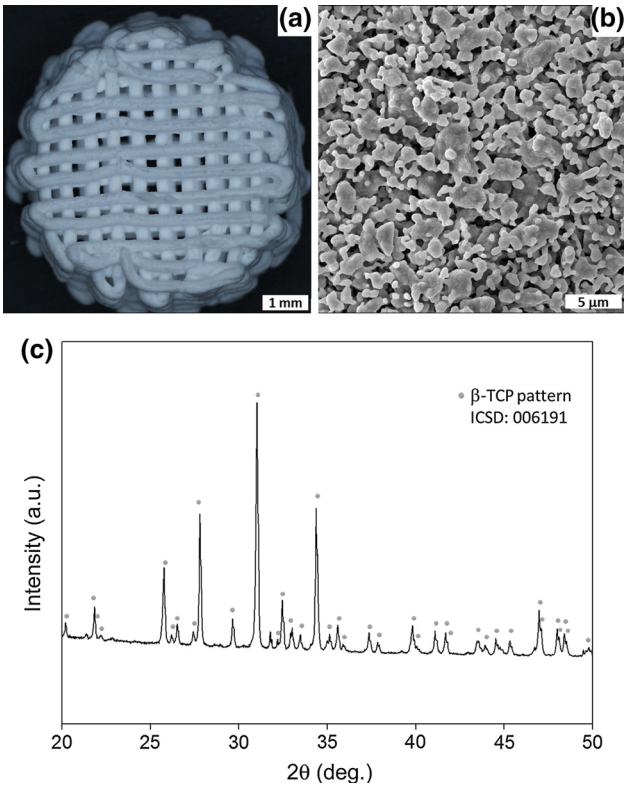

Fig. 1 Microstructure and composition of sintered robocast preforms. **a** TCP preform produced by direct ink writing with a controlled macro-porosity of 350 μm, **b** microstructure of TCP preform after sintering at 1100 °C per 5 h, **c** XRD of TCP preform after sintering

close to the head. It is important to underline that the excess of magnesium is important to prevent that pores due to magnesium solidification appear inside the preform.

After cutting, the sample was observed that magnesium penetrates all the macro-pores in the TCP preform (Fig. 2b), forming a continue matrix that envelops the TCP filaments. This is a significant advantage for the mechanical properties of the material, because the metallic component can toughen the ceramic component, driving to an improved mechanical strength [32].

The microstructure of the Mg–TCP composite revealed two main components (Fig. 3a). One phase is the TCP ceramic meanwhile the second phase is the metal. Detailed observation of the metallic component revealed that it is composed by magnesium and Mg–Ca precipitates (Fig. 3b, d) that according with EDX have a chemical stoichiometry equivalent to $CaMg_2$. The presence of the Mg–Ca intermetallic was corroborated by EDX in Fig. 4, where the elemental mapping analysis shows the presence of calcium in the magnesium phase where the intermetallic microstructure of $CaMg_2$ is located. Moreover, some porosity was observed in the samples after their metallographic preparation (Fig. 3a). Pores in the position of the

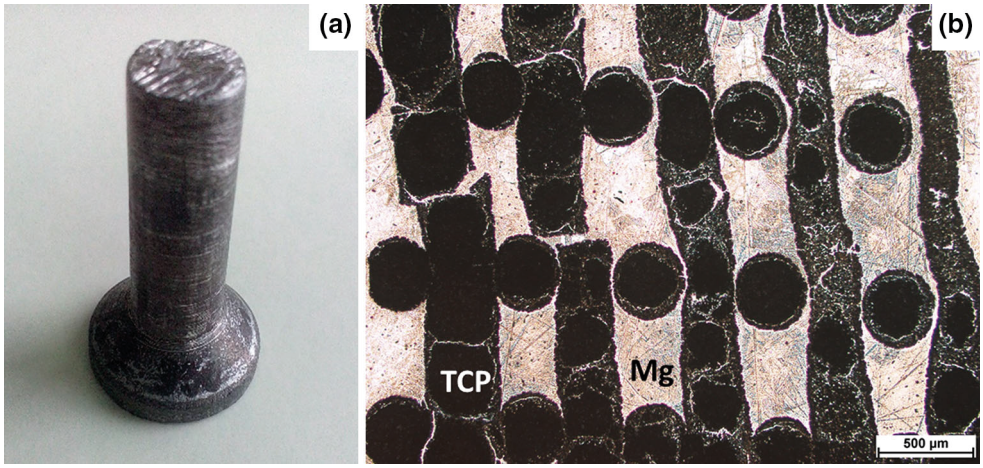

Fig. 2 TCP preform after CAMI. **a** screw-like specimen from a TCP preform infiltrated with Mg, **b** optical microscopy image of the interpenetrated Mg–TCP composite obtained by CAMI

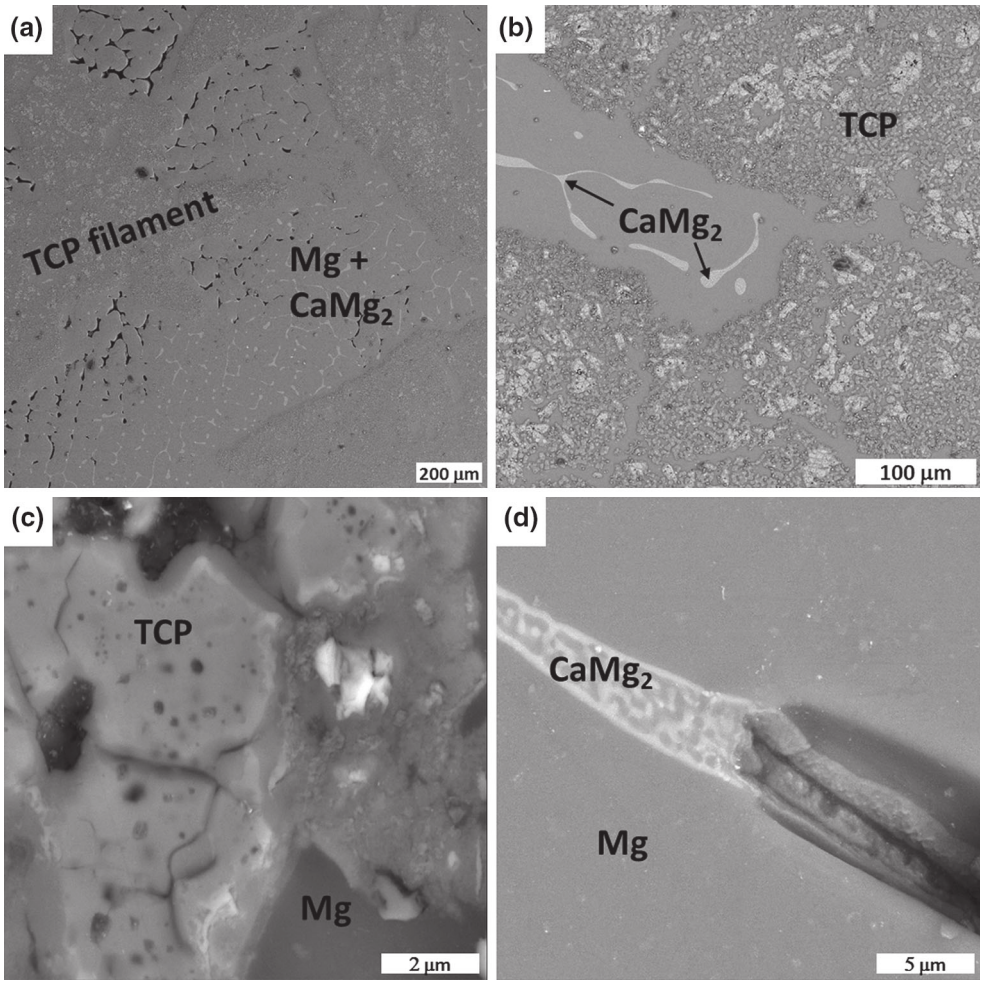

Fig. 3 SEM images of Mg–TCP interpenetrated composite. **a** Overall view of the Mg–TCP composite, **b** the presence of $CaMg_2$ intermetallic, **c** close-up of the ceramic phase, **d** close-up of the Mg + $CaMg_2$ intermetallic

intermetallic are attributed to spallation of the intermetallic from the magnesium matrix during metallographic preparation of the samples. This is based on the fact that the porosity has the same shape and is aligned to the intermetallic microstructure, as it can be observed in Fig. 3d. One possible explanation for the formation of the

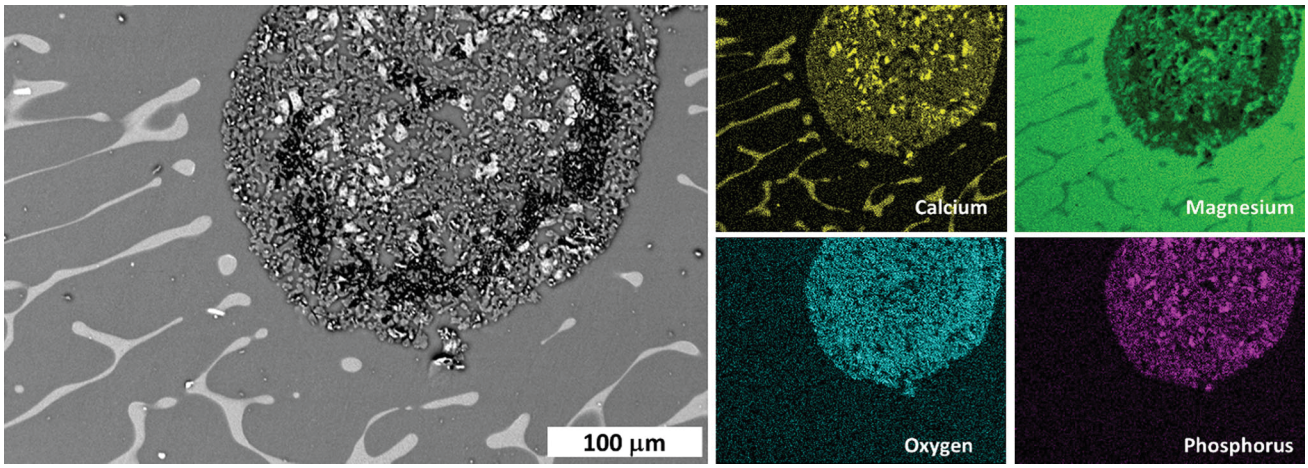

Fig. 4 Elemental chemical analysis by EDX of Mg–TCP interpenetrated composite

intermetallic is the partial release and dissolution of calcium in the molten magnesium during infiltration. In fact, magnesium can dissolve up to 1.34 wt% of Ca (at 789.5 K) according with the Mg–Ca binary phase diagram [33]. It has been reported that the invariant reaction in the Mg-rich region occurs at 10.5 ± 0.5 at.% Ca and at 790 K [34], then it can be easily expected that the $CaMg_2$ eutectic phase is formed during the heating and infiltration process.

The ceramic component shows the infiltration of magnesium even inside the micro-pores of the TCP filaments (pores below 2 µm), referring to a good infiltration process (Fig. 3b, c). The presence of magnesium inside of the TCP filaments is corroborated by EDX in Fig. 4. Nonetheless, the TCP filaments still present some closed porosity as it can be observed in Fig. 3c.

In Fig. 5, XRD shows that the crystalline structure of the filaments was TCP. This means that although some dissolution of calcium into magnesium was observed, the TCP crystalline structure was preserved. It might be expected that the loss of calcium atoms from TCP could lead on the partial phase transformation or decomposition of the TCP; however, no characteristics peaks of other phases were recognized by XRD (Fig. 5). This is a signal of no chemical reactions during infiltration although the high reactivity of magnesium. Nonetheless, it is probable that ionic diffusion occurred during sintering leading on the substitution of calcium with magnesium in the TCP crystalline lattice. In fact, magnesium is considered as a stabilizer of the beta phase of TCP [35]. Furthermore, Mg–TCP interface seems to be well defined, as it can be appreciated in all the micrographies in Fig. 3. XRD analysis of the Mg–TCP composite confirmed the existence of $CaMg_2$ observed by SEM (Fig. 5). Besides, although the infiltration and heat treatment were carried out under vacuum, a partial oxidation of magnesium was observed by XRD (Fig. 5).

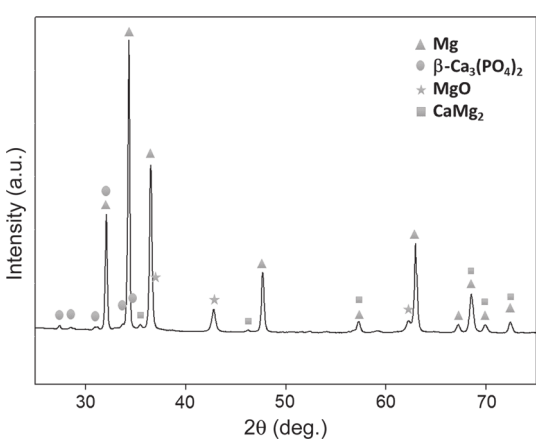

Fig. 5 XRD pattern for Mg–TCP interpenetrated composite obtained by CAMI

Figure 6a shows some of the composite samples for the degradation test in saline solution. Figure 6b shows a Mg–TCP disc with corrosion products after 24 h of immersion, while in Fig. 6c, the same sample after removal of corrosion products can be observed. The estimated degradation rates in mm $year^{-1}$ are shown in Fig. 7.

Results show that for pure magnesium, after 6 h in saline solution, it presents the highest DR (135.6 mm $year^{-1}$), meanwhile for the composite, the highest value is registered after 3 h (40.8 mm $year^{-1}$). Afterwards, for both materials, the DR decreases till reaching the lowest rate after 24 h of immersion, being a final value of 52.4 and 12 mm $year^{-1}$ of DR for pure magnesium and for the composite, respectively (Fig. 7). The reduction in the DR is attributed to the formation of a MgOH layer on the surface of the samples which impair sample corrosion [33, 36].

The DR within the first 24 h revealed a higher degradation rate for pure magnesium in comparison with the Mg–TCP composite (Fig. 7). Therefore, the infiltration of TCP with magnesium significantly reduced the DR of the

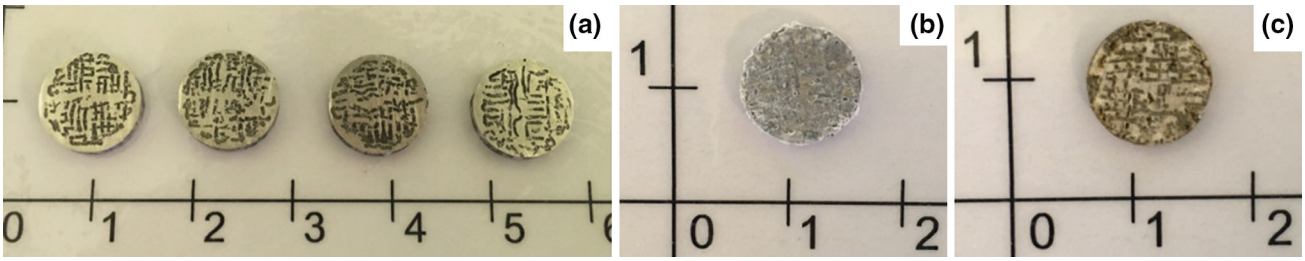

Fig. 6 Representative samples for degradation test. **a** Mg–TCP composite discs for degradation test, **b** Mg–TCP composite disc after 24 h of degradation test in saline solution, **c** same Mg–TCP sample than **b** after the removal of corrosion products with CrO_3 and $AgNO_3$

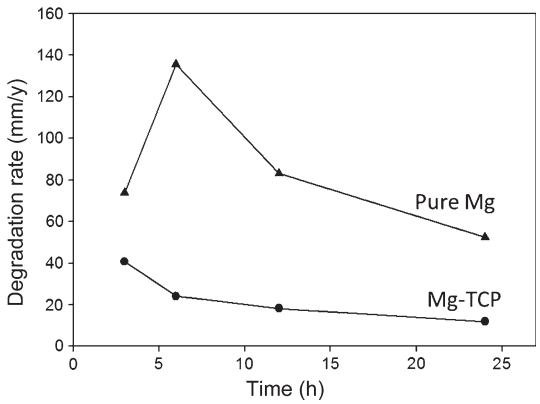

Fig. 7 Degradation rates over the time for pure magnesium and Mg–TCP composite

material. Nonetheless, the DR of the composite continues being outside the required value for functional treatment of bone defects [37]. Calcium phosphate coatings are proposed as a further approach to improve the corrosion resistance of the composite [38–40]. In addition to the less magnesium surface exposed to the liquid environment, the reduction in the DR of the composite can result from the formation of the $CaMg_2$ intermetallic, because generally, magnesium alloys are investigated for decrement in the degradation rate of magnesium. Mg–Ca alloys have been studied for such approaches [9–12, 33]. On the other hand, galvanic micro-corrosion can be expected between intermetallic and magnesium, due to their potential difference; nevertheless, due to the faster formation of the protective layer when Mg–Ca alloy is present, it might be one of the reasons why in the composite the DR is lower than the one for pure magnesium [33, 41].

4 Conclusions

1. The manufacturing of interpenetrated composites combining advanced techniques such as direct ink writing and CAMI is an excellent and novel method for the development of new advanced materials in the diverse areas of the science and industry. Fragile materials, such as porous robocast TCP preforms, can be successfully and fully infiltrated with magnesium through CAMI technique. Due to the presence of magnesium in both macro-pores and micro-pores of the TCP preforms, it can be assumed that the infiltration technique proposed in this research can be consider as a virtuous technique for metal infiltration.
2. The resulted Mg–TCP composite has shown a well-defined and continuous interface between the ceramic and metallic phase. Possible dissolution of calcium into the molten magnesium during the infiltration is assumed after the formation of the $CaMg_2$ intermetallic, present in all the volume where the TCP scaffold is situated. Nevertheless, no chemical degradation of TCP is detected by XRD, what is attributed to some atomic substitution between the magnesium and calcium atoms.
3. From the results of the degradation test and in accordance with the literature, the DR of magnesium-based materials under isotonic saline solution at 37 °C is followed by a decrease in the corrosion rate as the time is increasing. The obtained interpenetrated composite has shown a degradation rate around 3 times slower than the one for pure magnesium.
4. As DR is a main concern in the application of magnesium-based implants, several strategies must be essayed to decelerate the degradation rate and therefore to guarantee the necessary mechanical properties during the bone healing time. TCP scaffolds infiltrated with high corrosion resistant magnesium alloys could be a good alternative to face this problem.

Acknowledgements This project has received funding from the European Union's Horizon 2020 research and innovation programme under the Marie Skłodowska-Curie, and it is co-financed by the South Moravian Region under Grant No. 665860. Authors also acknowledge the project CEITEC 2020 (LQ1601) with financial support from the Ministry of Education, Youth and Sports of the Czech Republic under the National Sustainability Program II. MCL acknowledges to Brno Ph.D. Talent scholarship founded by the Brno City Municipality. SDT acknowledges to Conacyt Mexico, through the project CB.177700, and COFAA-IPN (SIP project 20144443).

References

[1] F. Witte, F. Feyerabend, P. Maier, J. Fischer, M. Stormer, C. Blawert, W. Dietzel, N. Hort, Biomaterials **28**, 2163 (2007)

[2] D. Pijocha, A. Zima, Z. Paszkiewicz, A. Ślósarczyk, Acta Bioeng. Biomech. **15**, 53 (2013)

[3] A.K. Khanra, H.C. Jung, S.H. Yu, K.S. Hong, K.S. Shin, Bull. Mater. Sci. **33**, 43 (2010)

[4] K. Mensah-Darkwa, R.K. Gupta, D. Kumar, J. Mater. Sci. Technol. **29**, 788 (2013)

[5] R.Z. LeGeros, J.P. LeGeros, Key Eng. Mat. **240–242**, 3 (2003)

[6] M.P. Staiger, A.M. Pietak, J. Huadmai, G. Dias, Biomaterials **27**, 1728 (2006)

[7] F. Witte, N. Hort, C. Vogt, S. Cohen, K.U. Kainer, R. Willumeit, F. Feyerabend, Curr. Opin. Solid State Mater. Sci. **12**, 63 (2008)

[8] F. Witte, Acta Biomater. **23**, S28 (2015)

[9] F. Witte, V. Kaese, H. Haferkamp, E. Switzer, A. Meyer-Lindenberg, C.J. Wirth, H. Windhagen, Biomaterials **26**, 3557 (2005)

[10] Y. Chen, Z. Xu, C. Smith, J. Sankar, Acta Biomater. **10**, 4561 (2014)

[11] A. Myrissa, N.A. Agha, Y. Lu, E. Martinelli, J. Eichler, G. Szakács, C. Kleinhans, R. Willumeit-Römer, U. Schäfer, A.M. Weinberg, Mater. Sci. Eng. **61**, 865 (2016)

[12] X. Gu, Y. Zheng, Y. Cheng, S. Zhong, T. Xi, Biomaterials **30**, 484 (2009)

[13] M. Bohner, Injury **31**, D37 (2000)

[14] H. Yuan, Z. Yang, Y. Li, X. Zhang, J.D. de Bruijn, K. de Groot, J. Mater. Sci. Mater. Med. **9**, 723 (1998)

[15] J. Lu, M. Descamps, J. Dejou, G. Koubi, P. Hardouin, J. Lemaitre, J.P. Proust, J. Biomed. Mater. Res. A **63**, 408 (2002)

[16] O. Gauthier, J.M. Bouler, E. Aguado, P. Pilet, G. Daculsi, Biomaterials **19**, 133 (1998)

[17] V. Karageorgiou, D. Kaplan, Biomaterials **26**, 5474 (2005)

[18] B.S. Chang, C.K. Lee, K.S. Hong, H.J. Youn, H.S. Ryu, S.S. Chung, K.W. Park, Biomaterials **21**, 1291 (2000)

[19] X. Miao, L.P. Tan, L.S. Tan, X. Huang, Mater. Sci. Eng. **27**, 274 (2007)

[20] J. Franco, P. Hunger, M.E. Launey, A.P. Tomsia, E. Saiz, Acta Biomater. **6**, 218 (2010)

[21] A.R. Akkineni, Y. Luo, M. Schumacher, B. Nies, A. Lode, M. Gelinsky, Acta Biomater. **27**, 264 (2015)

[22] A. Butscher, M. Bohner, S. Hofmann, L. Gauckler, R. Müller, Acta Biomater. **7**, 907 (2011)

[23] J.A. Lewisw, J.E. Smay, J. Stuecker, J. Cerarano, J. Am. Ceram. Soc. **89**, 3599 (2006)

[24] P. Miranda, A. Pajares, E. Saiz, A.P. Tomsia, F. Guiberteau, J. Biomed. Mater. Res. A **85**, 218 (2008)

[25] S. Michna, W. Wua, J.A. Lewis, Biomaterials **26**, 5632 (2005)

[26] P. Miranda, E. Saiz, K. Gryn, A.P. Tomsia, Acta Biomater. **2**, 457 (2006)

[27] D.R. Clarke, J. Am. Ceram. Soc. **75**, 739 (1992)

[28] A. Mattern, B. Huchler, D. Staudenecker, R. Oberacker, A. Nagel, M.J. Hoffmann, J. Eur. Ceram. Soc. **24**, 3399 (2004)

[29] K.M.S. Manu, L.A. Raag, T.P.D. Rajan, M. Gupta, B.C. Pai, Metall. Mater. Trans. B **47**, 2799 (2016)

[30] S. Grasso, Y. Sakka, G. Maizza, Sci. Technol. Adv. Mater. **10**, 053001 (2009)

[31] R. Orru, R. Licheri, A.M. Locci, A. Cincotti, G. Cao, Mater. Sci. Eng., R **63**, 127 (2009)

[32] K. Konopka, M.C. Maj, K.J. Kurzydlowski, Mater. Charact. **51**, 335 (2003)

[33] Z. Li, X. Gu, S. Lou, Y. Zheng, Biomaterials **29**, 1329 (2008)

[34] Alloy Phase Diagram, *In: ASM handbook*, vol. 3 (ASM International, The Materials Information Company, Geauga County, 1992)

[35] A. Gozalian, A. Behnamghader, M. Daliri, A. Moshkforoush, Sci. Iran. F **18**, 1614 (2011)

[36] I. Rocnáková, E.B. Montufar, M. Horynová, T. Zikmund, K. Novotný, L. Klakurková, L. Celko, G.L. Song, J. Kaiser, Corros. Sci. **104**, 187 (2016)

[37] F. Shapiro, Eur. Cells Mater. **15**, 53 (2008)

[38] S. Shadanbaz, G.J. Dias, Acta Biomater. **8**, 20 (2012)

[39] F.Z. Cui, J.X. Yang, Y.P. Jiao, Q.S. Yin, Y. Zhang, I.S. Lee, Front. Mater. Sci. China **2**, 143 (2008)

[40] L. Xu, F. Panc, G. Yu, L. Yang, E. Zhang, K. Yang, Biomaterials **30**, 1512 (2009)

[41] G.L. Song, A. Atrens, Adv. Eng. Mater. **1**, 11 (1999)